Fully implicit numerical integration of a hyperelastoplastic model for sands based on critical state plasticity

J.E. Andrade*, R.I. Borja

Stanford University, Department of Civil and Environmental Engineering, Stanford, CA 94305, USA

Abstract

This paper deals with the numerical implementation of a hyperelastoplastic model for sands based on critical state theory (CST). Additional features introduced in the model capture sand behavior more realistically but also introduce new challenges in the numerical implementation of the model. We demonstrate that a fully implicit algorithm is achievable by showing how consistent linearization of the residual vectors results in a solution algorithm exhibiting asymptotic quadratic rate of convergence. We perform two representative numerical examples, at a stress point, to demonstrate the robustness of the proposed implicit scheme.

Keywords: Critical state theory; Hyperelastoplasticity; Implicit integration; Geomechanics

1. Introduction

Models based on critical state theory for soils have received significant attention in the geotechnical community due to their ability to capture soil behavior adequately. A new hyperelastoplastic non-associative model for sands based on CST has been formulated by Borja and Andrade [1]. What mainly distinguishes this new model from the more classic Cam-Clay models, such as that presented in [2], is the introduction of a state parameter ψ_i which allows the yield surface to detach from the critical state line, and a hardening law, which depends on the state of stress, the state parameter ψ_i, and the deviatoric plastic stresses. The upshot of this is a strong coupling between the size parameter p_i and ψ_i. We demonstrate, mostly by means of examples, how the model is still amenable to a fully implicit implementation exhibiting optimal rate of convergence. We follow the notations in [1] where a more ample discussion about the model can be found.

2. The hyperelastoplastic model

Consider a particular strain energy function of the form $\psi = \psi(\varepsilon_v^e, \varepsilon_s^e)$, where the independent variables are the infinitesimal volumetric and deviatoric elastic strain invariants. From the Coleman–Noll relationships, and only considering mechanical energy, the Cauchy stress tensor is obtained by $\boldsymbol{\sigma} = \partial\psi/\partial\boldsymbol{\varepsilon}^e$.

Consider now the first two invariants of the Cauchy stress tensor p and q, which we can use to postulate the following yield surface:

$$F(p, q, p_i) = q + \eta p \leq 0 \tag{1}$$

where

$$\eta = \begin{cases} M[1 + \ln(p_i/p)] & N = 0 \\ (M/N)\left[1 - (1-N)(p/p_i)^{N/(1-N)}\right], & N > 0 \end{cases} \tag{2}$$

The parameter $p_i < 0$ is called the image stress that controls the size of the yield surface, and $N \geq 0$ is a constant material parameter governing the curvature of the yield surface and typically has a value less than 0.4 for sands. The material constant M is prescribed such that $\eta = -q/p = M$ when $p = p_i$ on the yield surface. A plastic potential function of the same form as the yield surface can be postulated by defining the parameters $\bar{p}_i$ and $\bar{N}$ as the non-associative counterparts of p_i and N, respectively. If $\bar{N} = N$ and $\bar{p}_i = p_i$, then plastic flow is said to be associative. Otherwise, the flow rule is non-associative in the volumetric sense.

Finally, the evolution of the size parameter is governed by a hardening law, which is a function of the

* Corresponding author. Tel.: +1 (650) 723 1502; Fax: +1 (650) 725 9255; E-mail: jandrade@stanford.edu

Computational Fluid and Solid Mechanics 2005
K.J. Bathe (Editor)

state of stress, the state parameter ψ_i, and the deviatoric plastic stresses. The parameter ψ_i allows the yield surface to detach from the critical state line, feature which previous Cam-Clay models do not have, and which allows this model to capture the dilative behavior of sands better. This hardening law naturally couples p_i with ψ_i, imposing additional challenges in the numerical treatment of the model.

3. Numerical implementation

Following [1], we consider a local residual vector emanating from a return mapping in strain invariant space [1,2]:

$$\mathbf{r}(\mathbf{x}) = \begin{Bmatrix} \varepsilon_v^e - \varepsilon_v^{e\,tr} + \Delta\lambda\beta\partial_p F \\ \varepsilon_s^e - \varepsilon_s^{e\,tr} + \Delta\lambda\partial_q F \\ F \end{Bmatrix}, \quad \mathbf{x} = \begin{Bmatrix} \varepsilon_v^e \\ \varepsilon_s^e \\ \Delta\lambda \end{Bmatrix} \tag{3}$$

where $\mathbf{x}$ is the vector of local unknowns, $\boldsymbol{\varepsilon}^{e\,tr}$ is the trial elastic strain tensor, which is assumed to be given, and $\beta = (1 - N) / (1 - \bar{N})$ is a non-associativity parameter. The system is then solved iteratively using a Newton-Raphson scheme with a Jacobian matrix of the form $\mathbf{r}'(\mathbf{x}) = \partial\mathbf{r}/\partial\mathbf{x}$. Consistently linearizing the residual vector in question yields optimal convergence results locally, and, ultimately, also globally. Additionally, as mentioned earlier, the coupling between the size parameter p_i and ψ_i requires additional iterations at a sub-local level, where given the total deformations we can solve for these two state variables simultaneously. Once the coupled parameters are obtained, we can then proceed with the solution to the next step.

In order to conserve the asymptotic rate of convergence in the FEM implementation or in stress-point stress-driven simulations, it is necessary to derive the consistent tangent operator (CTO), $\mathbf{c} = \partial\boldsymbol{\sigma}/\partial\boldsymbol{\varepsilon} \equiv \partial\boldsymbol{\sigma}/\partial\boldsymbol{\varepsilon}^{e\,tr}$. We do so by recalling the residual vector described above but increasing the number of unknowns such that the trial elastic strain tensor itself becomes an unknown at the global level. This procedure yields an algorithmic tangent operator exhibiting asymptotic quadratic rate of convergence as illustrated in the following numerical examples.

4. Representative numerical examples

We perform two representative numerical examples to show the robustness of the algorithm presented above. The first simulation deals with a sample of dense sand with the material parameters $N = 0.4$ and $\bar{N} = 0.2$, and loaded with prescribed strains $\Delta\varepsilon_{11} = 5 \times 10^{-4}$ and $\Delta\varepsilon_{22} = \Delta\varepsilon_{33} = -1/2\Delta\varepsilon_{11}$. We use this strain-controlled simulation to show the rate of convergence of the return mapping algorithm at the *local* level. Figure 1 shows convergence profiles at various load-steps for the sample in question. It can be observed that the rate of convergence is asymptotically quadratic at every step shown, and that convergence is achieved within five iterations or less. This trend was observed at all load-steps in the simulation.

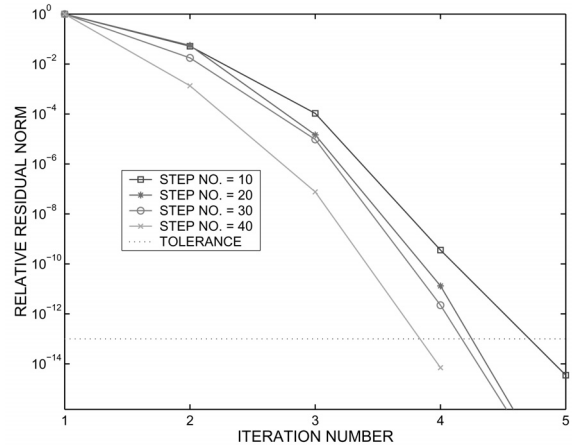

Fig. 1. Convergence profile of local Newton iterations for isochoric strain-controlled simulation on a sand specimen with $N = 0.4$ and $\bar{N} = 0.2$.

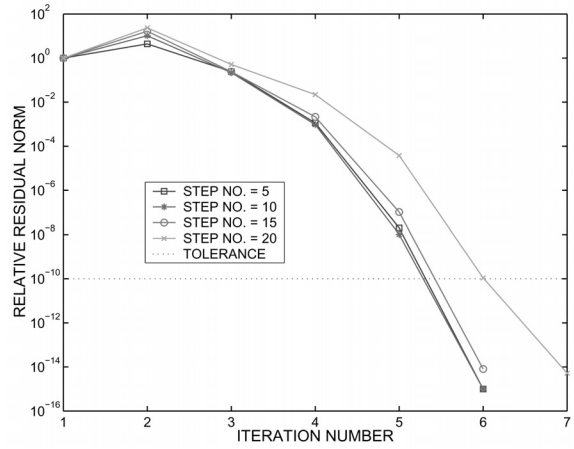

Fig. 2. Convergence profile of global Newton iterations for stress-controlled simulation on a sand specimen with $N = 0.4$ and $\bar{N} = 0.2$.

The second simulation pertains to a stress-controlled test on the same soil sample described above. This simulation provides information about the convergence rate at the *global* level using the CTO. The loading protocol consists of keeping the mean normal stress constant at $p = -130\,\text{kPa}$ and varying the initially nil

deviatoric stress with $\Delta q = 7.5\,\text{kPa}$. Figure 2 shows the convergence profile of the global residual vector at various load steps. As in the case of the strain-controlled simulation, each of the steps shown in the figure displays asymptotic quadratic rate of convergence. All load-steps in this simulation showed the same trend.

5. Conclusion

We have presented the numerical implementation of a novel hyperelastoplastic model based on critical state theory for sands. Careful treatment of the state variables involved in the problem allows us to solve the problem implicitly without sacrificing any desirable quality inherited from the return mapping algorithm. Specifically, we have shown that consistent linearization leads to asymptotic quadratic rate of convergence, both locally and globally.

Acknowledgments

This work has been supported by the US National Science Foundation under grant numbers CMS-0201317 and CMS-0324674.

References

[1] Borja RI, Andrade JE. Critical state plasticity, part VI: meso-scale finite element simulation of strain localization in discrete granular materials. Comp Meth in App Mech and Eng, In review for the John Argyris Memorial Special Issue.

[2] Borja RI, Tamagnini C. Cam-Clay plasticity, part III: extension of the infinitesimal model to include finite strains. Comput Methods Appl Mech Eng 1998;155:73–95.